
Proceedings Paper:
Saechan, P, Mao, X and Jaworski, AJ (2015) Optimal design of a thermoacoustic system comprising of a standing-wave engine driving a travelling-wave cooler. In: Proceedings of ICR2015. ICR2015 : The 24th IIR International Congress of Refrigeration, 16-22 Aug 2015, Yokohama, Japan. International Institute of Refrigeration.

ID:514

OPTIMAL DESIGN OF A THERMOACOUSTIC SYSTEM COMPRISING OF A STANDING-WAVE ENGINE DRIVING A TRAVELLING-WAVE COOLER

Patcharin SAECHAN(*), Xiaoan MAO(**) and Artur J. JAWORSKI(**)

(*) Department of Mechanical and Aerospace Engineering, Faculty of Engineering, King Mongkut's University of Technology North Bangkok, 10800, Thailand
(**) Faculty of Engineering, University of Leeds, Leeds LS2 9JT, United Kingdom
a.j.jaworski@leeds.ac.uk

ABSTRACT

This paper presents the design and optimisation of a coupled thermoacoustic system comprising of a standing wave thermoacoustic engine and a coaxial travelling wave thermoacoustic cooler in a linear configuration. The overall aim is to propose an economical design of a prototype system which could be used by people living in remote rural areas of developing countries with no access to the electrical grid. The cooler coaxial configuration provides a feedback inertance and compliance to create the required travelling-wave phasing. Compressed air at 10 bar is used as the working fluid. The operating frequency is around 50 Hz. The geometric parameters of both engine and cooler, affecting the overall efficiency of cooling, have been investigated to evaluate the optimal configuration of the system. The most sensitive parameters are the cross sectional areas of the engine and cooler and the hydraulic radii of stack and regenerator.

1. INTRODUCTION

Thermoacoustics is a field of study dealing with the conversion between thermal and acoustic energies in working fluids in the vicinity of solid boundaries. Usually, environmentally friendly inert gases or air are used as working fluids. When a thermoacoustic cooler is driven by a thermoacoustic engine, a potentially very attractive device with no moving parts and little maintenance cost can be engineered (Garett *et al.,* 1993). Thermoacoustic devices are classified into "engines/prime movers" and "refrigerators/coolers" depending on the practical implementation of the thermoacoustic effect. The thermoacoustic engine converts thermal energy into an acoustic energy. Conversely, the thermoacoustic cooler uses an acoustic wave to induce a heat pumping effect which in turn generates a temperature gradient. The thermoacoustic devices can also be grouped into "standing wave" and "travelling wave" devices, depending on whether acoustic pressure and acoustic velocity are 90 degrees out of phase or in phase, respectively (Swift, 1988).

As a result of attempts over three decades, the energy conversion efficiency of the thermoacoustic devices has been increasing rapidly, one of the most effective designs being that of Backhaus and Swift (2000). The travelling wave thermoacoustic engine was developed with a high thermal efficiency of about 30%. Here, an inherently reversible Stirling cycle is employed to achieve a large acoustic power with minimum viscous loss. It consists of a loop tube connected to a long resonator pipe. However, it seems to be inconvenient for practical use due to a bulky shape. A coaxial configuration is an alternative which is more compact and has relatively high performance (Tijani and Spoelstra, 2008). An acoustic network based on the same principle as a torus-shaped design, providing high acoustic impedance in the regenerator, is employed in this configuration.

Current work is based on an early practical demonstrator that involved coupling a thermoacoustic engine to a thermoacoustic cooler in a single unit (Saechan *et al.,* 2012), and earlier modelling dealing mainly with the cooler part alone as described in Saechan *et al.* (2011), which enabled the build. The overall aim was to show the feasibility of a cooler for storing essential medicines for rural communities with no access to the electric grid and thus the principles of such a system had to be proven in the laboratory. However, admittedly, the resulting device such as shown by Saechan *et al.* (2012) would be too large and heavy to be used in practice.

Therefore, further improvements in terms of the performance and practical build are required before final implementation in rural communities through mass production. This paper extends previous work by performing a series of simulations, which are conceptually similar to those described by Saechan et al. (2011) for the cooler alone, but importantly they subject the parameters of both the engine and cooler to the optimisation process and in particular "free" the device diameter. In addition, the optimisation now looks at the overall cooling efficiency instead of being limited to COP of the cooler alone.

2. CONCEPTUAL DESIGN AND SIMULATION

In this paper, the design and optimisation of a coupled system of thermoacoustic engine and cooler is presented. A standing wave thermoacoustic engine (SWTE) is selected to convert the heat energy into the acoustic power because of the uncomplicated structure of the straight line configuration. Coupled to the SWTE would be the travelling wave thermoacoustic cooler (TWTC) which consumes the acoustic power in order to pump heat against a temperature gradient and thus produces the refrigeration effect. Providing high efficiency of energy conversion from acoustic to thermal is the major advantage of using TWTC configuration. In order to retain the linear configuration, the cooler will be of coaxial type.

As outlined in the introduction section, in the previous work no attempt has been made to systematically study all the important geometrical parameters of both engine and the cooler subsystems simultaneously. In the current work, the values of many geometrical parameters, previously “assumed” for convenience of using standard components (e.g. the resonator diameter of six inch), have been treated as independent variables in order to investigate if a more compact (and ultimately lightweight) design of the demonstrator device is possible.

Such system is designed to operate with compressed air at 10 bars and frequency of 50 Hz. Briefly, main components of SWTE are: a stack, two heat exchangers and a resonator, as shown in Figure 1. The stack for the engine is a layered parallel-plate stainless steel because of the simplicity of fabrication. The central part of the TWTC is the regenerator which consists of stacked-up layers of stainless steel mesh screens with a small hydraulic radius compared to the thermal penetration depth ($r_h << \delta_\kappa$). Therefore, a very good thermal contact between the gas and solid in the regenerator can be achieved; the temperature of the gas can be assumed to be the same as the temperature of the adjacent solid. All heat exchangers in both SWTE and TWTC are designed as parallel plate configuration with the working gas oscillating between the plates.

In the design of the TWTC, the cooling temperature of 250 K at the cold heat exchanger is the target. The TWTC employs an acoustic network based on the same principle as the torus-shaped design (Tijani and Spoelstra, 2008). It consists of a feedback inertance, compliance and acoustic resistance as also shown schematically in Figure 1. The regenerator and heat exchangers generate an acoustic flow resistance. The annular space between the resonator and the regenerator holder forms the feedback inertance. The cylindrical volume of gas confined between the closed end of the resonator and the right side of the holder shapes the acoustic compliance. The acoustic network is designed to create the travelling wave phasing necessary to operate the thermoacoustic Stirling cycle and helps to create high acoustic impedance in the regenerator. The acoustic power produced by SWTE is delivered to TWTC. It is consumed to pump heat from the low temperature to the high temperature end of the regenerator in the TWTC.

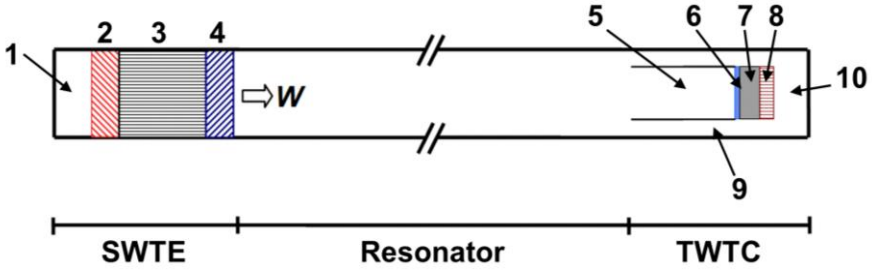

Figure 1. The schematic diagram of the coupled system: (1) bounce space (BS), (2) hot heat exchanger (HHX), (3) stack (STK), (4) ambient heat exchanger (AHX_{SWTE}), (5) thermal buffer tube (TBT), (6) cold heat exchanger (CHX), (7) regenerator (REG), (8) ambient heat exchanger (AHX_{TWTC}), (9) inertance tube, (10) compliance

The design and optimisation are implemented based on the linear thermoacoustic theory, which assumes that the device geometry and flow of energy are one-dimensional and along a path extending from one termination to another along the central axis of gas oscillation. The fundamental physics concerned with the linear thermoacoustics theory can be described by the continuity, energy and momentum equations which are the functions of temperature, angular frequency, pressure and volume flow rate amplitudes, system geometry and gas properties (Swift, 2002). The changes in pressure amplitude (p_1), velocity amplitude (U_1), mean temperature (T_m) and total power flow rate ($\dot{H}$) along a thermoacoustic segment can be determined as presented below:

$$\frac{dp_1}{dx} = -\frac{i\omega\rho_m}{(1-f_\nu)A}U_1 \tag{1}$$

$$\frac{dU_1}{dx} = -\frac{i\omega A}{\rho_m a^2}\left[1+\frac{(\gamma-1)f_\kappa}{1+\varepsilon_s}\right]p_1 + \frac{\beta(f_\kappa-f_\nu)}{(1-f_\nu)(1-\sigma)(1+\varepsilon_s)}\frac{dT_m}{dx}U_1 \tag{2}$$

$$\frac{dT_m}{dx} = \frac{\dot{H}_2 - \frac{1}{2}\mathrm{Re}\left[p_1\tilde{U}_1\left(1-\frac{T_m\beta(f_\kappa-\tilde{f}_\nu)}{(1+\varepsilon_s)(1+\sigma)(1-\tilde{f}_\nu)}\right)\right]}{\frac{\rho_m c_p|U_1|^2}{2A\omega(1-\sigma)|1-f_\nu|^2}\mathrm{Im}\left(\tilde{f}_\nu+\frac{(f_\kappa-\tilde{f}_\nu)(1+\varepsilon_s f_\nu/f_\kappa)}{(1+\varepsilon_s)(1+\sigma)}\right)-Ak-A_{solid}k_{solid}} \tag{3}$$

$$\begin{aligned}\dot{H}_2 = {} & \frac{1}{2}Re\left[p_1\tilde{U}_1\left(1-\frac{T_m\beta(f_\kappa-\tilde{f}_\nu)}{(1+\varepsilon_s)(1+\sigma)(1-\tilde{f}_\nu)}\right)\right] \\ & + \frac{\rho_m c_p|U_1|^2}{2A\omega(1-\sigma)|1-f_\nu|^2}\frac{dT_m}{dx}Im\left[\tilde{f}_\nu+\frac{(f_\kappa-\tilde{f}_\nu)(1+\varepsilon_s f_\nu/f_\kappa)}{(1+\varepsilon_s)(1-\sigma)}\right]-(Ak+A_{solid}k_{solid})\frac{dT_m}{dx}\end{aligned} \tag{4}$$

where ω is angular frequency, a, ρ_m, T_m, c_p, γ, k, β and σ are speed of sound, mean density, temperature, isobaric specific heat capacity, ratio of specific heats, thermal conductivity, gas expansion coefficient and Prandtl number of working fluid, respectively. A is flow area of the channel. i is imaginary unit. Re, Im and superscript ~ denote the real part, imaginary part and conjugation of a complex quantity, respectively. f_ν, f_κ and ε_s are viscous function, thermal function and correction factor for finite solid heat capacity, respectively, depending on the geometry of individual components (Ward *et al.*, 2008). The acoustic power produced or dissipated in any segment per unit length can be estimated as (Swift, 2002):

$$\frac{d\dot{W}_{AC}}{dx} = \frac{1}{2}\mathrm{Re}\left[\tilde{U}_1\frac{dp_1}{dx}+\tilde{p}_1\frac{dU_1}{dx}\right] \tag{5}$$

Due to the TWTC being driven by the SWTE in this work, the overall system efficiency (referred to as "overall efficiency of cooling" here) is seemingly the best description of the overall performance of the device as it combines the performance of both SWTE and TWTC. It can be written as:

$$\eta_{cooling} = \frac{\dot{Q}_C}{\dot{Q}_H}. \tag{6}$$

where $\dot{Q}_C$ is heat load of the TWTC and $\dot{Q}_H$ is the input heat power supplied by the hot heat exchanger of the SWTE. Additionally, the above parameter is employed to justify the design choices in the pursuit of the optimal design.

The design and performance analysis were aided by the simulation programme DeltaEC (Ward *et al.*, 2008). This computer code is widely used to design and predict the efficiency of the thermoacoustic engines and refrigerators. The one-dimensional wave equations based on low-amplitude approximation are solved simultaneously to determine the change of the variables of state of the working fluid (for example oscillatory pressure, oscillatory volume flow rate, acoustic power flow, total power flow etc.) along all segments of a thermoacoustic device. With a geometry given by the user, a solution found in each segment is required to match at the junctions the solutions for the neighbouring segments. In simulation, the proposed system in Figure 1 can be characterised as block diagram as illustrated in Figure 2. The calculation begins at the

bounce space (BS) segment and then ends at hard end segment which is the usual part of a closed thermoacoustic system.

When defining the boundaries for the simulation, the volumetric velocity must become zero at the main tube ends due to rigid walls:

$$U_1 = 0 \text{ at } x = 0, x = L, \tag{7}$$

L being the main resonator length. According to the momentum and acoustic power equations, these boundary conditions result in:

$$\frac{\partial p_1}{\partial x} = 0 \text{ and } \dot{W}_{AC} = 0 \text{ at } x = 0, x = L \tag{8}$$

Due to the flow split at the beginning of the TWTC, the flow criteria are then set up to ensure that complex pressure amplitude and temperature at the union point of the main component trunk and the inertance branch are the same. These conditions are:

$$p_{1,Trunk} = p_{1,Branch} \text{ and } T_{Trunk} = T_{Branch} \tag{9}$$

For the volumetric velocity at the "union", the condition is of course flow continuity:

$$U_{1,Resonator} = U_{1,Trunk} + U_{1,Branch}\,. \tag{10}$$

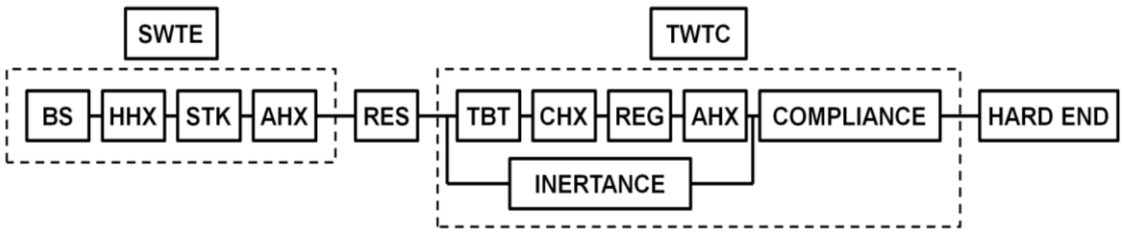

Figure 2. The component arrangement of the system presented as block diagram

3. OPTIMISATION PROCEDURE

In the optimisation process, the boundary conditions are set up and initially, the geometries of each component in Figure 2 are assumed. The solutions are then guessed in order to meet the targets by solving the differential momentum, continuity, and total power equations simultaneously as described above. Fourth-order Runge-Kutta integration method is employed in the DeltaEC design code. If the solutions diverge, the guessed values are then adjusted and re-calculated until the convergence is achieved. The shooting method is used in this work to find the guess values which are consistent with target results. In the first converged solutions, the efficiency of the system obtained is typically quite low, as may be expected, because the geometries of the thermoacoustic device have not been optimised. Therefore, the optimisation process is subsequently executed to achieve the maximum efficiency of the entire system based on the multivariable search method. The optimisation procedure is performed by varying the values of the parameters in each component of the SWTE, including the cross sectional area, the plate spacing and the length of the stack, the plate spacing and the length of the heat exchangers. The parameters involved in the optimisation process of the TWTC are the length and the hydraulic radius of the regenerator, cooler diameter, the lengths of thermal buffer tube and the heat exchangers and the compliance volume. The optimisation process stops, when the optimal configuration of both SWTE and TWTC is achieved giving the maximum overall efficiency of cooling. Table 1 shows the investigated ranges of parameters during the SWTE and TWTC parametric optimisation.

However, some parameters are kept constant in this work due to the limitations of the manufacturing and cost effectiveness in design. These parameters are input power at SWTE, plate thickness of the stack and the solid temperature of both ambient heat exchangers. The 600 W of input power at SWTE is employed in the model which is comparable to the heat supplied by the anticipated biomass combustion process. Moreover, the plate thickness of 0.2 mm in the stack is the thinnest in the market at a reasonable price. Although a thinner stack plate thickness may yield a higher efficiency, one must take into account reasonable costs of

the thermoacoustic device as one of the main objectives of the current design. The solid temperature of ambient heat exchangers in both SWTE and TWTC are assumed 300 K which corresponds to the cooling fluid temperature. To avoid the effect of the entrance losses, the porosity of the heat exchangers is assumed to be equal to that for the stack (Tijani *et al.*, 2002). In addition, ideal thermal insulation around the thermoacoustic device is assumed, thus the heat interactions with the surroundings are assumed to take place only through the heat exchangers. As has been reported by Swift (2002), the optimal length of the heat exchanger can be determined from the peak-to-peak displacement amplitude of the gas at the heat exchanger location, corresponding to the distance within which the working fluid transfers heat between the stack and heat exchanger. This guideline is taken into account in the optimised simulation.

Table 1. Investigated parameters of SWTE and TWTC

Standing Wave Engine (SWTE)			
Component	**Parameter (unit)**	**Range**	**Optimised value**
Hot heat exchanger (HHX)	Length (mm)	10-50	23.03
	Plate spacing (mm)	1-10	1.46
Stack (STK)	Length (mm)	50-500	370
	Plate spacing (mm)	0.3-1.2	0.52
Ambient heat exchanger (AHX)	Length (mm)	20-100	62.41
	Plate spacing (mm)	1-10	1.15
Diameter of the SWTE	Length (mm)	80-150	93
Travelling Wave Cooler (TWTC)			
Component	**Parameter (unit)**	**Range**	**Optimised value**
Cold heat exchanger (CHX)	Length (mm)	5-15	11.4
	Plate spacing (mm)	0.5-5	0.5
Regenerator (REG)	Length (mm)	10-70	26
	Hydraulic radius (μm)	10-60	40.71
Ambient heat exchanger (AHX)	Length (mm)	5-15	12.4
	Plate spacing (mm)	0.5-5	0.5
Thermal buffer tube (TBT)	Length (mm)	10-120	68
Compliance volume	Length (mm)	10-200	168
Diameter of the TWTC	Length (mm)	50-87	79.6

4. RESULTS AND DISCUSSION

Figure 3 illustrates the results obtained from DeltaEC. The pressure and volumetric velocity amplitude distributions along the system are shown for the final optimised case. Overall, the system exhibits a half-wavelength behaviour; the velocity nodes are at the ends and the pressure node is located in the centre. There is a pressure drop along the SWTE stack caused by the flow resistance of the stack. At the "union" (junction) point near the TWTC front (where inertance branch separates from TBT "trunk"), the oscillatory volumetric velocity separates into two components. In order to balance the pressure drop across the TWTC, the larger component is present at the inlet of the inertance tube due to a low resistance while the smaller component is present at the inlet to the TBT as the regenerator present in this branch constitutes a higher flow obstruction. This effect can be seen on the pressure amplitude distribution as a pressure drop at the regenerator.

Further discussion will focus on the influence of the individual parameters affecting the cooling performance of the TWTC driven by the SWTE. The variation of the cooling efficiency against the dimensionless geometry which is normalised by its optimised dimension is presented in Figure 4. The optimal geometry ratio equals unity at the maximum cooling performance. Thus, this represents the sensitivity of the overall efficiency of cooling of the entire system to each parameter of SWTE and TWTC.

4.1. Effect of SWTE geometric parameters

As can be seen in Figure 4(a), the cross sectional area of the SWTE and plate spacing of the stack have the most significant effect on the overall efficiency of cooling. The diameter of the SWTE which is the outer border of the feedback inertance tube has a significant effect on acoustic power flow in TWTC. This will be

discussed later. As is well known, the porosity of the stack is the key factor in the acoustic power generation, and this porosity is also represented in terms of stack plate spacing and will be discussed later on. In contrast, the overall efficiency of cooling is almost insensitive to the plate spacing variation of heat exchangers. The details of each parameter affecting the efficiency of the cooler will be discussed below.

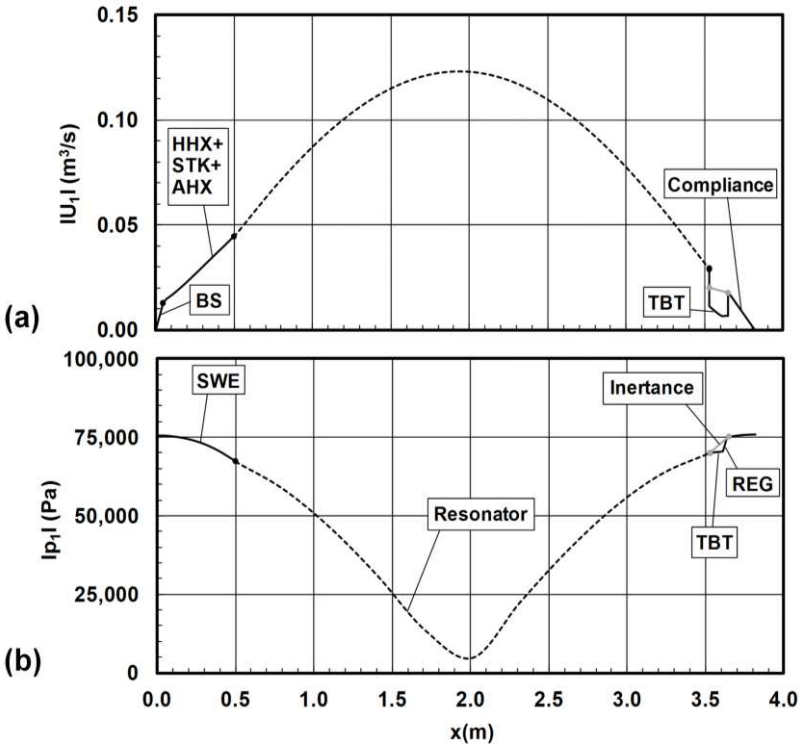

Figure 3. Pressure (a) and volumetric velocity (b) amplitude distribution along the system

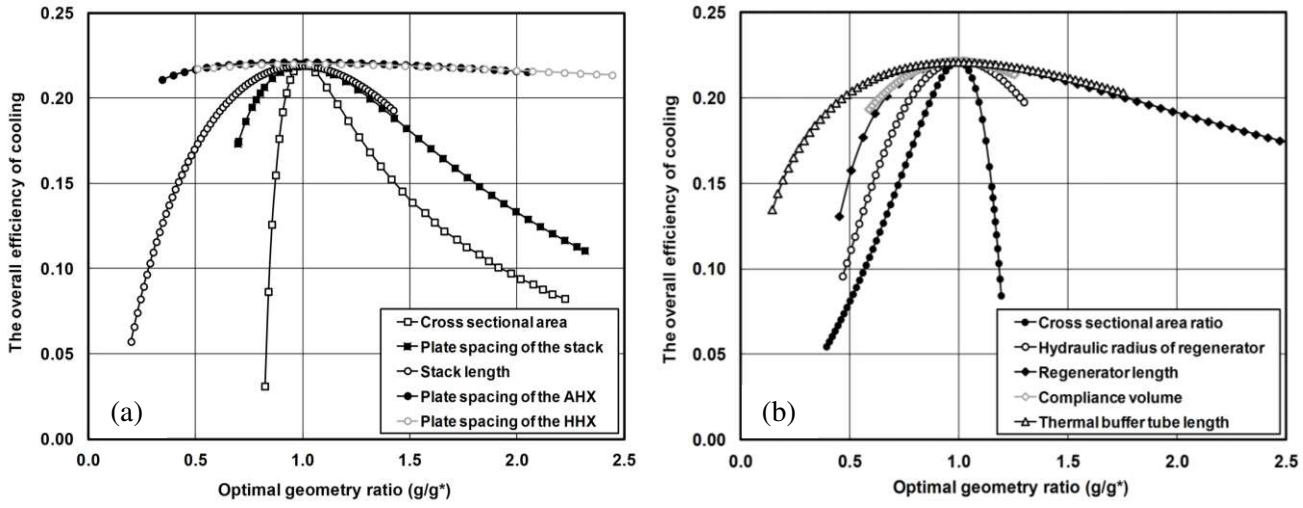

Figure 4. Effects of geometric parameters on the overall efficiency of cooling: (a) SWTE, (b) TWTC

The stack composes of multiple plates aligned parallel to the resonator tube. The most critical parameter of the stack is its hydraulic radius (r_h) which is the ratio of the cross sectional area and the perimeter of the channel or the ratio of the gas volume to the gas-solid contact area. In parallel plate stack design, the hydraulic radius is equivalent to half the plate spacing (y_0) (Tijani *et al.*, 2002). The plate spacing establishes the degree of thermal interaction between the gas flowing between the plates and the stack material which is the kind of interaction that needs to be optimised to obtain the maximum performance. If the gaps are too narrow, the viscous effects will cause the gas to lose too much energy to friction. If the gaps are too large, the gas cannot effectively transfer heat to and from the solid material in the stack.

The next parameter to be considered is the length of the stack. The effect of the length of the stack on the overall efficiency of cooling would be a direct proportionality as the increased stack length enhances the

acoustic power generation (Swift, 2002). However, when the stack is too long, there will be a significant dissipation, which also reduces the overall efficiency of cooling.

The cross sectional area of the engine is the total area including the area of gas and solid. The generated acoustic power from the stack is also directly proportional to the cross sectional area (Swift, 2002). Due to the assumed constant heat input into the engine, the increase of the cross sectional area is limited to produce the maximum acoustic power.

Heat exchangers are the necessary components in the thermoacoustic device to supply and extract heat at the ends of the stack. Here, the length and the plate spacing of the heat exchangers will be discussed. The optimum length is determined from the movement of gas at the heat exchanger location from the peak to peak displacement amplitude (equal to $2|U_1|/\omega$). It approximates the axial distance of a gas parcel moving in one cycle of oscillation which is proportional to the volumetric velocity amplitude at the given frequency. The effect of the plate spacing of heat exchangers on acoustic power is similar to that of plate spacing in the stack. The optimal configurations which provide the maximum overall efficiency are presented in Table 1.

4.2. Effect of TWTC geometric parameters

The significant parameters of cooler affecting the overall efficiency of cooling are illustrated in Figure 4(b). Again, the overall efficiency of cooling is extremely sensitive to the cross sectional area ratio and the hydraulic radius of regenerator, while the change of thermal buffer tube length has a small effect on overall efficiency of cooling. The cross sectional area ratio is the ratio of the regenerator holder cross sectional area to the total cross sectional area. The acoustic power consumption of the regenerator of TWTC is directly proportional to the cross sectional area (Swift, 2002). However, the cooling capacity of the TWTC has to be a compromise between the area of the cooler and inertance tube (i.e. the annular space) to obtain the maximum cooling capacity because the feedback inertance space is also needed to return the acoustic power to the cooler and adjust the phase difference between the oscillating pressure and volumetric velocity to operate the reversed Stirling cycle in the TWTC.

The hydraulic radius (r_h) indicates the level of the thermal contact between working fluid and solid in the regenerator. If the hydraulic radius is small, perfect thermal contact between working fluid and solid wall will be realised. However, then the pressure drop across the regenerator increases considerably, which results in a low volume flow rate amplitude and cooling performance.

The increase of regenerator length enhances the acoustic power consumption and reduces the temperature gradient across the regenerator. The overall efficiency of cooling decreases rapidly as the regenerator length is less than the optimum value. This might be due to the fixed temperature gradient across the regenerator as the design target. Thus, as the regenerator length decreases, the acoustic consumption also decreases resulting in smaller cooling capacity.

The compliance cavity is provided by the volume of gas enclosed at the end of the TWTC acting as the space for the feedback acoustic power returning to the cooler unit. The increased volume of the compliance leads to an increase of volume flow rate amplitude resulting in higher cooling capacity. However, a larger volume of the compliance will give a negative effect in acoustic power dissipation and reduce the acoustic power flow to the cooler.

The thermal buffer tube is located between the cold heat exchanger and the flow straightener of the TWTC and used as a thermal cushion. The temperature of air then rises gradually from the cooling temperature to mean temperature along the thermal buffer tube. It can be seen that the variation of thermal buffer tube length has a smaller effect on the overall efficiency of cooling comparing to other parameters.

From this it can clearly be inferred that the areas of SWTE and TWTC, and the hydraulic radii of stack and regenerator are the vital parts in the simulations of the coaxial thermoacoustic cooler driven by the thermoacoustic engine and then a careful design must be undertaken due to the sensitivities found. In the design of thermoacoustic devices, there are many geometrical solutions to achieve the workable devices as shown by the results above, but only one solution actually is the optimum to match the given criteria. In this work, the design of thermoacoustically driven thermoacoustic cooler to accomplish the maximum cooling

performance at temperature of 250 K is carried out systematically leading to an optimal configuration from the point of view of the overall cooling efficiency. The simulation results are summarised in Table 2. Optimisation process leads to the final model with optimised parameters presented earlier in Table 1.

Table 2. Simulation results of the design of TWTC driven by SWTE

Parameters	Results
The maximum acoustic power conversion efficiency of the SWTE	17%
Acoustic pressure amplitude	0.775 bar
Drive ratio	7.75%
The cooling capacity at cooling temperature of 250 K	133 W
COP	1.9
The overall efficiency of cooling	22.2%

5. CONCLUSIONS

A detailed numerical study of the coaxial travelling wave thermoacoustic cooler driven by the standing wave thermoacoustic engine has been discussed in this study. The main objective of this work was to find the optimal design of a device which could be utilised for providing a cooling capability for storing vital medical supplies in remote and rural areas based on thermoacoustic technology. The compressed air at 10 bar pressure is selected to be the working gas and the operating frequency of 50 Hz is chosen. The value of geometrical parameters of the engine and the cooler are considered. The design and optimisation lead to the design of a compact device giving more cooling capacity. The cooling temperature of 250 K at TWTC and input power of 600 W at the hot heat exchanger of SWTE have been the targets of this design. It is apparent from the optimisation results that the drive ratio of 7.75% can be produced by the SWTE with the thermal-to acoustic energy conversion efficiency of 17.0%. The cooling load of 133 W (kept the same as in Saechan et al. (2011) for benchmarking purposes) can be extracted from the optimised system which is equivalent to COP of 1.9. The overall efficiency of cooling can reach the maximum of 22.2%. These predictions represent an improvement over the existing practical build (Saechan *et al*. 2012) which provided the maximum overall efficiency of only 4% at the cooling temperature of 278 K. In addition, this design provides a more compact and lightweight system (in practice the diameter of 93 mm can be implemented using less standard but available pipe diameters of 3.5 or 3.75 inch. It also produces more acoustic power compared to the existing demonstrator. Further work will focus on the construction of the improved prototype including the implementation of the hot heat exchangers driven by hot gases from the combustion process.

6. REFERENCES

Garrett SL, Hofler TJ, Perkins DK. 1993, Thermoacoustic Refrigeration, *Refrigeration and Air conditioning Technology Workshop*, C51-58.

Swift GW. 1988, Thermoacoustic engines, *J. Acoust. Soc. Am.* 84 (4): 1146-80.

Backhaus S, Swift GW. 2000, A thermoacoustic-Stirling heat engine: Detailed study, *J. Acoust. Soc. Am.* 107(6): 3148-66.

Tijani MEH, Spoelstra S. 2008, Study of a coaxial thermoacoustic-Stirling cooler, *Cryogenics* 48(1): 77–82.

Saechan P, Yu Z, Jaworski AJ. 2012, Design and experimental evaluation of a travelling wave thermoacoustic cooler driven by a standing wave thermoacoustic engine, *Proc. 19th ICSV, 2012.*

Saechan P, Yu Z, Jaworski AJ. 2011, Optimal design of coaxial travelling wave thermoacoustic cooler, *Proc. 23th IIR* International *Congress of Refrigeration, ICR2011:* ID 590.

Swift GW. 2002, *A unifying perspective for some engines and refrigerators*, Acoustical Society of America Publications, Melville, NY.

Ward B, Clark J, Swift GW. 2008, Design Environment for Low-Amplitude ThermoAcoustic Energy Conversion program, Los Alamos National Laboratory, New Mexico, USA.

Tijani MEH, Zeegers JCH, de Waele ATAM. 2002, Design of thermoacoustic refrigerators, *Cryogenics* 42 (1): 49–57.